Contribution from the Department of Chemistry, University of Calgary, Calgary, Alberta, Canada T2N 1N4, and Instituto de Física e Química de São Carlos, Universidade de São Paulo, 13560 São Carlos, S.P., Brazil

Comparison of the Electronic Structures and Electrochemical Reduction of the P_3N_3, $P_2SN_3^+$, PS_2N_3, and $S_3N_3^-$ Rings:[1] X-ray Crystal Structures of $(Ph_2PN)_2(NSX)$ (X = Cl, I, NMe_2, Ph)

N. BURFORD,[†] T. CHIVERS,*[†] M. HOJO,[†] W. G. LAIDLAW,*[†] J. F. RICHARDSON,[†] and M. TRSIC[‡]

Received August 13, 1984

The crystal structures of $(Ph_2PN)_2(NSX)$ (**5a**, X = Cl; **5b**, X = I; **5c**, X = NMe_2; **5d**, X = Ph) have been determined by X-ray crystallography. The crystal data are as follows: for **5a**·CH_3CN, monoclinic, space group $P2_1$, a = 11.376 (4) Å, b = 7.512 (1) Å, c = 14.808 (6) Å, β = 95.99 (2)°, V = 1259 Å^3, and Z = 2; for **5b**·CH_3CN, monoclinic, space group $P2_1$, a = 11.451 (2) Å, b = 7.710 (1) Å, c = 15.335 (3) Å, β = 95.69 (1)°, V = 1347 Å^3, and Z = 2; for **5c**, monoclinic, space group $P2_1/n$, a = 9.902 (2) Å, b = 9.612 (1) Å, c = 25.882 (5) Å, β = 90.265 (8)°, V = 2463 Å^3, and Z = 4; for **5d**, monoclinic, space group $C2/c$, a = 23.771 (1) Å, b = 13.999 (1) Å, c = 19.220 (1) Å, β = 123.617 (6)°, V = 5326 Å^3, and Z = 8. In **5d** the six-membered P_2SN_3 ring is planar to within 0.08 Å whereas the sulfur atom in **5a**, **5b**, and **5c** lies out of the NPNPN plane by 0.30, 0.29, and 0.55 Å, respectively. The exocyclic sulfur–halogen bond lengths of 2.357 (2) and 2.713 (3) Å for **5a** and **5b**, respectively, are ca. 15% longer than the sum of the covalent radii for sulfur and the halogens. Pronounced inequalities are observed for the P–N bond lengths in **5a** and **5b**. In the PNP units the average values are 1.580 (4) (**5a**) and 1.586 (4) Å (**5b**) compared to 1.667 (5) and 1.662 (9) Å for the P–N bond lengths in the PNS units. This difference is much smaller for **5d** (1.596 (3), 1.618 (2) Å) and almost negligible for **5c** (1.594 (2), 1.606 (2) Å). The average endocyclic S–N bond lengths are significantly shorter in **5a** (1.554 (4) Å) and **5b** (1.550 (7) Å) compared to **5c** (1.595 (3) Å) and **5d** (1.618 (3) Å). Ab initio Hartree–Fock–Slater SCF calculations on the model compound $(H_2PN)_2(SN)^+$ show that (a) the $P_2SN_3^+$ ring contains six cyclic π electrons, (b) the π bonding is localized primarily in the NSN and PNP segments of the ring and is relatively weak for the P–N bonds connecting these units, (c) the LUMO is strongly antibonding with respect to the NSN unit, (d) the energies of the planar and half-chair ring conformations are similar, but the S–N bonds are strengthened when the sulfur atom is lifted out of the plane, and (e) the first electronic transition should be in the region of 300 nm. The electronic structure of the $P_2SN_3^+$ ring (**2**) is compared with those of the related six-membered rings, P_3N_3 (**1**), PS_2N_3 (**3**), and $S_3N_3^-$ (**4**). The electrochemical reduction potentials of **1**–**4** correlate well with $\epsilon(\pi$ LUMO) – ϵ(LOMO) for these four heterocycles.

Introduction

All four members of the series of inorganic heterocycles containing alternating phosphorus or sulfur and nitrogen atoms, **1**–**4**,

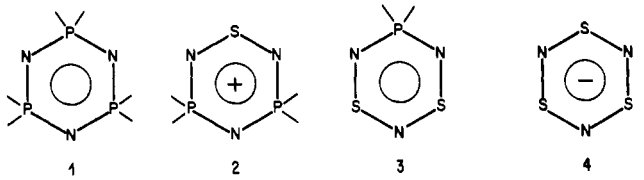

1 **2** **3** **4**

are now known.[2] The P_3N_3 ring system (**1**) is characterized by high thermal stability and resistance to oxidation or reduction, and potential applications in medicine or catalysis have been demonstrated for various derivatives.[3] By contrast the π-electron-rich $S_3N_3^-$ ring (**4**)[4] is thermally unstable[5] and readily oxidized.[6,7] The hybrid ring system **3** is formally derived from **4** by replacement of an S atom by R_2P^+, and it retains the characteristics of a cyclothiazene.[8,9] Similarly **2** is derived from **1** by substitution of S^+ fo an R_2P group. However, the properties of **2** differ from those of the cyclophosphazene (**1**) in two important respects.

The first difference concerns the structure of the heterocyclic ring. The P–N bonds connecting the PNP and NSN units in **2** are considerably longer (1.66–1.67 Å) than the P–N bonds in the PNP unit itself (1.58–1.59 Å).[10–13] The second dissimilarity is related to the chemical reactivity of **2**. This heterocycle readily undergoes ring opening via rupture of an S–N bond under the influence of nucleophiles or reducing agents. For example, the chloro derivative of **2** is converted to 12-membered rings by Me_3SiNMe_2[14] or by triphenylantimony at 23 °C.[15] The reagent $Me_3SiNSNSiMe_3$ also takes part in a ring-expansion reaction via insertion of the sulfur diimide bridge into the S–N bonds of **2** to give eight-membered rings.[11] The short S–N bond lengths (ca. 1.56 Å)[11,12] are indicative of a substantial π-bonding contribution in **2** (cf. d(S–N) ~ 1.55 Å in $S_4N_4^{2+}$, which possesses a strongly π-bonded framework).[16] Thus, at first sight, the rupture of the heterocyclic ring in **2** via cleavage at S–N, in preference to the long, connecting P–N bonds, is surprising.

In order to understand these facets of the chemistry of the $P_2SN_3^+$ ring we have determined the X-ray crystal structures of two covalent derivatives of **2**, **5c** (X = NMe_2) and **5d** (X = Ph).

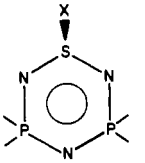

5a, X = Cl
b, X = I
c, X = NMe_2
d, X = Ph

(1) Throughout this paper the ring systems are represented only by their endocyclic atoms; the two exocyclic substituents on each phosphorus atom have been omitted for simplicity.
(2) Chivers, T. *Acc. Chem. Res.* **1984**, *17*, 166.
(3) Allcock, H. R. *Adv. Chem. Ser.* **1983**, *No. 232*, 49.
(4) Bojes, J.; Chivers, T.; Laidlaw, W. G.; Trsic, M. *J. Am. Chem. Soc.* **1979**, *101*, 4517.
(5) Chivers, T.; Laidlaw, W. G.; Oakley, R. T.; Trsic, M. *J. Am. Chem. Soc.* **1980**, *102*, 5773.
(6) Chivers, T.; Cordes, A. W.; Oakley, R. T.; Pennington, W. T. *Inorg. Chem.* **1983**, *22*, 2429.
(7) Chivers, T.; Rao, M. N. S. *Can. J. Chem.* **1983**, *61*, 1957.
(8) Burford, N.; Chivers, T.; Cordes, A. W.; Laidlaw, W. G.; Noble, M.; Oakley, R. T.; Swepston, P. N. *J. Am. Chem. Soc.* **1982**, *104*, 1282.
(9) Burford, N.; Chivers, T.; Oakley, R. T.; Oswald, T. *Can. J. Chem.* **1984**, *62*, 712.
(10) These bond lengths refer to derivatives of **2** that have an exocyclic halogen ligand (Cl^{11} or I^{12}) attached to sulfur. The long sulfur–halogen bond lengths are indicative of a substantial cationic character for the ring in these derivatives.
(11) Chivers, T.; Rao, M. N. S.; Richardson, J. F. *J. Chem. Soc., Chem. Commun.* **1982**, 982.
(12) Chivers, T.; Rao, M. N. S.; Richardson, J. F. *J. Chem. Soc., Chem. Commun.* **1983**, 700.
(13) Pohl, S.; Petersen, O.; Roesky, H. W. *Chem. Ber.* **1979**, *112*, 1545.
(14) Chivers, T.; Rao, M. N. S.; Richardson, J. F. *J. Chem. Soc., Chem. Commun.* **1983**, 702.
(15) Chivers, T.; Rao, M. N. S.; Richardson, J. F. *J. Chem. Soc., Chem. Commun.* **1983**, 186.
(16) (a) Gillespie, R. J.; Kent, J. P.; Sawyer, J. F.; Slim, D. R.; Tyrer, J. D. *Inorg. Chem.* **1981**, *20*, 3799. (b) Trsic, M.; Laidlaw, W. G.; Oakley, R. T. *Can. J. Chem.* **1982**, *60*, 2281.

[†] University of Calgary.
[‡] Universidade de São Paulo, São Carlos.

0020-1669/85/1324-0709$01.50/0

Table I. Crystallographic Parameters for $(Ph_2PN)_2(NSX)$[a]

	X			
	Cl	I	NMe_2	Ph
fw	520.5	612.14	488.5	521.6
space group	$P2_1$	$P2_1$	$P2_1/n$	$C2/c$
a, Å	11.376 (4)	11.451 (2)	9.902 (2)	23.771 (1)
b, Å	7.512 (1)	7.710 (1)	9.612 (1)	13.999 (1)
c, Å	14.808 (6)	15.335 (3)	25.882 (5)	19.220 (1)
β, deg	95.99 (2)	95.69 (1)	90.265 (8)	123.617 (6)
V, Å^3	1259	1347	2463	5326
Z	2	2	4	8
D_{calcd}, g cm^{-3}	1.37	1.51	1.32	1.30
radiation	Cu Kα Ni prefilter	Mo Kα graphite monochromated	Mo Kα graphite monochromated	Cu Kα Ni prefilter
temp, °C	−100 (5)	23 (1)	23 (1)	23 (1)
scan range ($\Delta\omega$), deg	1.5(0.54 + 0.142 tan θ)	1.5(0.60 + 0.347 tan θ)	1.5(0.54 +0.347 tan θ)	1.5(0.54 + 0.142 tan θ)
scan speed, deg min^{-1} (variable)	1.7–6.7	0.7–6.7	0.5–5	0.6–5
max θ, deg	75	30	27.5	70
no. of reflcns scanned	2805	4178	5635	5042
no. of obsd reflcns ($I > 3\sigma(I)$)	2749	1729	1618	3423
cryst dimens, mm^3	0.53 × 0.35 × 0.30	0.44 × 0.36 × 0.23	0.37 × 0.23 × 0.16	0.40 × 0.36 × 0.28
μ, cm^{-1}	34.34	14.20	2.84	23.52
weighting formula $[\sigma^2(F_o) + n(F_o)^2]^{-1}$	$n = 0.001$	$n = 0.0$	$n = 0.0$	$n = 0.003$
no. of observns used in final cycle	2749	2910[b]	3479[b]	3423
no. of variables	306	306	298	326
max residual ed, e Å^{-3}	0.60	0.93	0.16	0.29
GOF	3.59	2.36	1.23	0.90
R, R_w[c]	0.047, 0.065	0.048, 0.040	0.035, 0.022	0.041, 0.051

[a] For X = Cl and I, crystals used in the structural determination contained one molecule of CH_3CN. [b] Observed data plus those for which $I_c > 3\sigma(I_o)$. [c] $R = \Sigma(||F_o| - |F_c||)/\Sigma|F_o|$; $R_w = [\Sigma w(|F_o| - |F_c|)^2/\Sigma w|F_o|^2]^{1/2}$.

We have also carried out simple Hückel and ab initio Hartree–Fock–Slater (HFS) SCF MO calculations for $P_2SN_3^+$ in order to determine the (π)-electronic structure of this heterocycle and to compare it with those of the related six-membered rings P_3N_3, PS_2N_3,[8] and $S_3N_3^-$.[4] Finally, we have measured the electrochemical reduction potentials of **1–4** and correlated them with the calculated energies of the LUMOs of these four ring systems, adjusted to account for the effect of charge.

Experimental Section

Synthesis. The compounds $(Ph_2PN)_2(NSX)$ (X = Cl,[11] I,[12] NMe_2,[14,17] Ph[17]) and $(Ph_2PN)(SN)_2$[8] were prepared according to literature procedures.

Physical Measurements. Details of the equipment and procedures used for the electrochemical measurements are described in ref 18. UV–visible spectra were obtained by use of a Cary 219 spectrophotometer.

Collection and Reduction of X-ray Data. The crystal data and experimental conditions are summarized in Table I. Cell constants and orientation matrices were determined by least-squares refinement of the diffraction geometry for 25 accurately centered high-angle reflections. The space groups were determined with use of the indexing routines of the diffractometer and by examination of the intensities measured during data collection. Ambiguous space group assignments were distinguished by the distribution of E values calculated with use of a K-curve.[19] The final choice of space group was confirmed in all cases by the successful solution and refinement of the structure. The intensity data were collected on an Enraf-Nonius CAD-4F automated diffractometer using an ω-2θ scan mode and were corrected for Lorentz and polarization effects. In the case of $(Ph_2PN)_2(NSPh)$ an absorption correction was applied. This correction was not possible for $(Ph_2PN)_2(NSCl)\cdot CH_3CN$ due to decomposition of the crystal after data collection. A correction was not considered necessary for **5b** and **5c**.

Structure Solution and Refinement. Atomic scattering factors for nonhydrogen atoms were taken from ref 20 and were corrected for the real and imaginary parts of the anomalous dispersion;[21] hydrogen atom scattering factors were taken from ref 22. The position of the I atom in $(Ph_2PN)_2(NSI)\cdot CH_3CN$ was readily located from a Patterson synthesis and the remainder of the structure determined by standard difference Fourier syntheses. Three structures (X = Cl, NMe_2, Ph) were solved by direct methods (MULTAN 78)[23]. All structures were refined by using full-matrix least-squares techniques as described previously.[24] All H atoms were located in areas of positive electron density in difference Fourier syntheses and were included in the model in idealized positions (sp^2, C–H = 0.95 Å, sp^3, C–H = 1.00 Å) with thermal parameters set to 1.1 times the effective isotropic thermal parameter of the bonded C atom. H atom parameters were not refined but were recalculated after each cycle of refinement. In the final cycles, all non-hydrogen atoms were refined with anisotropic thermal parameters and final difference Fourier synthesis showed only minor residual peaks that were of no chemical significance.

Theoretical Method. The Hartree–Fock–Slater self-consistent field (HFS SCF) method[25] was used to calculate the molecular orbitals. We have used this method for a number of sulfur–nitrogen systems,[4,16b] and more recently it has been applied to sulfur–nitrogen–phosphorus systems.[8] A double-ζ basis set, augmented with d orbitals on sulfur and phosphorus, is utilized and a single determinant state function is calculated.

Results and Discussion

X-ray Crystal Structures of $(Ph_2PN)_2(NSX)$ (5: X = Cl, I, Ph, NMe_2). The crystal structures of **5a–5d** consist of discrete molecular units with no unusual molecular contacts. The final atomic coordinates of the unique non-hydrogen portion of the molecules are given in Tables II–V. Thermal parameters, parameters for the hydrogen atoms, bond distances and bond angles for the exocyclic substituents in **5a–5d** and the list of structure factors are available as supplementary material.

(17) Chivers, T.; Rao, M. N. S. *Inorg. Chem.* **1984**, *23*, 3605.
(18) Chivers, T.; Hojo, M. *Inorg. Chem.* **1984**, *23*, 1526.
(19) Computing was performed at the University of Calgary with use of the X-RAY 76 package of crystallographic programs: Stewart, J. M., Ed. Technical Report TR-446; Computer Science Center: University of Maryland, College Park, MD, 1976.
(20) Cromer, D. T.; Mann, J. B. *Acta. Crystallogr., Sect. A: Cryst. Phys., Diffr., Theor. Gen. Crystallogr.* **1968**, *A24*, 321.
(21) "International Tables for X-ray Crystallography"; Kynoch Press: Birmingham, England, 1974; Vol. IV, p 149.
(22) Stewart, R. F.; Davidson, E.; Simpson, W. *J. Chem. Phys.* **1968**, *42*, 3175.
(23) Main, P.; et. al. "MULTAN 78"; University of York: York, England, 1978. In fact, **5a** and **5b** are isostructural.
(24) Burford, N.; Chivers, T.; Rao, M. N. S.; Richardson, J. F. *Inorg. Chem.* **1984**, *23*, 1946.
(25) Baerends, E. J.; Ellis, D. E.; Ros, P. *Chem. Phys.* **1973**, *2*, 41.

Table II. Positional Parameters ($\times 10^4$) and B_{eq} ($\times 10$) for the Non-Hydrogen Atoms of $(Ph_2PN)_2(NSCl)\cdot CH_3CN$

atom	x/a	y/b	z/c	B_{eq}, Å^2
Cl	3049 (1)	4939 (2)	4119 (1)	21
S	2356 (1)	5823[a]	2631 (1)	12
P(1)	808 (1)	2938 (2)	2100 (1)	10
P(2)	3248 (1)	2917 (2)	1718 (1)	11
N(1)	1100 (3)	4984 (6)	2506 (2)	14
N(2)	2006 (3)	2008 (6)	1770 (2)	12
N(3)	3302 (3)	5043 (6)	2059 (2)	15
N(4)	2418 (4)	620 (8)	6627 (3)	29
C(7)	2811 (5)	397 (8)	5971 (4)	29
C(8)	3356 (8)	99 (13)	5138 (5)	54
C(1)	283 (4)	1634 (7)	2947 (3)	13
C(2)	−146 (4)	2407 (7)	3707 (3)	16
C(3)	−663 (4)	1323 (8)	4314 (3)	17
C(4)	−758 (4)	−498 (7)	4169 (3)	17
C(5)	−327 (5)	−1265 (8)	3411 (4)	22
C(6)	197 (5)	−192 (8)	2806 (3)	21
C(11)	−254 (4)	3153 (7)	1173 (3)	13
C(12)	−1332 (4)	3981 (7)	1295 (3)	16
C(13)	−2202 (4)	4115 (8)	563 (3)	18
C(14)	−2006 (4)	3452 (8)	−277 (3)	18
C(15)	−946 (4)	2612 (7)	−397 (3)	15
C(16)	−70 (4)	2443 (7)	331 (3)	15
C(21)	3606 (3)	2984 (7)	568 (3)	12
C(22)	4609 (4)	2168 (7)	288 (3)	15
C(23)	4792 (4)	2168 (7)	−626 (3)	17
C(24)	3963 (4)	2958 (9)	−1262 (3)	19
C(25)	2978 (4)	3798 (8)	−985 (3)	19
C(26)	2796 (4)	3812 (7)	−76 (3)	16
C(31)	4366 (4)	1731 (7)	2397 (3)	14
C(32)	5534 (4)	2380 (8)	2532 (3)	18
C(33)	6376 (4)	1444 (8)	3084 (3)	20
C(34)	6073 (4)	−124 (8)	3500 (3)	19
C(35)	4921 (4)	−783 (8)	3369 (3)	20
C(36)	4072 (4)	156 (7)	2811 (3)	15

[a] Coordinate fixed to define the origin.

Table III. Positional Parameters ($\times 10^4$) and B_{eq} ($\times 10$) for the Non-Hydrogen Atoms of $(Ph_2PN)_2(NSI)\cdot CH_3CN$

atom	x/a	y/b	z/c	B_{eq}, Å^2
I	3194 (1)	5000[a]	4169 (5)	65
S	2343 (2)	5791 (3)	2502 (2)	33
P(1)	899 (2)	2920 (4)	2037 (2)	28
P(2)	3235 (2)	2945 (4)	1640 (2)	26
N(1)	1107 (5)	4932 (12)	1420 (4)	31
N(2)	2016 (5)	2008 (9)	1700 (4)	25
N(3)	3258 (5)	5009 (12)	1940 (4)	29
N(4)	2438 (13)	754 (18)	6551 (10)	94
C(7)	2740 (15)	458 (20)	5904 (12)	82
C(8)	3075 (15)	33 (29)	5093 (10)	127
C(1)	346 (8)	1674 (13)	2888 (6)	28
C(2)	−69 (9)	2385 (14)	3607 (6)	37
C(3)	−566 (10)	1338 (17)	4194 (7)	48
C(4)	−607 (10)	−409 (18)	4074 (8)	50
C(5)	−211 (11)	−1177 (16)	3359 (9)	60
C(6)	263 (9)	−133 (19)	2759 (6)	52
C(11)	−232 (7)	3066 (12)	1146 (6)	27
C(12)	−1312 (8)	3921 (14)	1263 (7)	41
C(13)	−2140 (8)	4033 (15)	563 (9)	50
C(14)	−1971 (9)	3407 (14)	−245 (8)	45
C(15)	−924 (10)	2592 (15)	−344 (6)	47
C(16)	−89 (9)	2376 (13)	333 (6)	34
C(21)	3591 (7)	2950 (13)	555 (5)	23
C(22)	4550 (8)	2073 (13)	264 (7)	33
C(23)	4762 (9)	2104 (14)	−612 (7)	41
C(24)	3974 (10)	2883 (15)	−1234 (6)	45
C(25)	3025 (9)	3789 (15)	−965 (7)	47
C(26)	2834 (8)	3822 (14)	−51 (7)	40
C(31)	4371 (8)	1851 (12)	2297 (6)	32
C(32)	5515 (8)	2462 (13)	2428 (7)	40
C(33)	6374 (9)	1669 (16)	2923 (8)	50
C(34)	6124 (8)	158 (22)	3339 (6)	54
C(35)	5003 (8)	−558 (13)	3248 (6)	49
C(36)	4140 (7)	325 (15)	2718 (5)	41

[a] Coordinate fixed to define the origin.

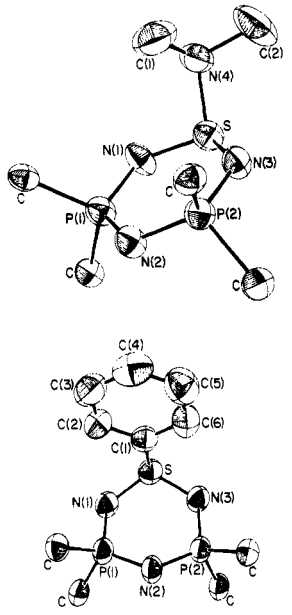

Figure 1. ORTEP drawings (50% probability ellipsoids) for $(Ph_2PN)_2(NSNMe_2)$ (**5c**) and $(Ph_2PN)_2(NSPh)$ (**5d**) showing the atomic numbering schemes. For clarity only the α-carbon atoms of the phenyl groups attached to phosphorus are shown. ORTEP drawings of **5a** and **5b** can be found in ref 11 and 12, respectively.

ORTEP drawings of **5c** and **5d** with the atomic numbering scheme are displayed in Figure 1, and the endocyclic bond lengths and angles for **5a–5d** are compared in Table VI. The best planes for the six-membered rings in **5a–5d** are given in Table VII. The P_2SN_3 ring is planar to within 0.08 Å in **5c** whereas for **5a**, **5b**, and **5d** the five-atom NPNPN units are approximately planar but the sulfur atom lies 0.30, 0.29, and 0.55 Å, respectively, out of this plane. The S–X bond vector makes angles of 93.0, 95.3, and 98.4° with the NPNPN plane in **5a**, **5b**, and **5d**, respectively, while in **5c** this angle is 121°.

For **5a** and **5b** the endocyclic bond angles at sulfur are ca. 117° compared ca. 113° in **5c** and **5d**. The endocyclic bond angles at phosphorus are in the range 114–118° typical for cyclophosphazenes.[26] The PNP bond angles are larger than the PNS angles (125° vs. 121°) in **5a** and **5b**, and a less pronounced difference is observed for **5d**. With **5c** the trend is reversed (120° for PNP vs. 126° for PNS). This difference is probably accounted for by the different ring geometry for **5c** (planar) compared to **5a**, **5b**, and **5d** (half-chair).

The exocyclic bond lengths of 2.357 (2) and 2.713 (3) Å for **5a** and **5b**, respectively, are indicative of significant ionic character in the S–X bonds (cf. sum of covalent radii for S and Cl is 2.03 and for S and I is 2.37 Å).[27] For **5d**, however, the corresponding bond length is 1.810 (3) Å, only slightly longer than a typical S–C_6H_5 bond (ca. 1.75 Å).[28] The exocyclic S–N bond length in **5c** of 1.685 (3) Å and the pyramidal geometry at N(4) (mean bond angle 112.1 (2)°) suggest that there is very little π bonding between the exocyclic nitrogen and sulfur in **5c** (cf. d(S–N) = 1.703 (3) Å and a mean bond angle at exocyclic nitrogen of 112.2 (4)° in the dimer $(Ph_2PN)_4(NSNMe_2)_2$).[14]

The mean endocyclic S–N bond lengths in $(Ph_2PN)_2(NSX)$ are shortest for **5a** and **5b** (1.558 (4) and 1.550 (7) Å, respectively), presumably as a result of the partial ionic character at sulfur. For **5c** and **5d** the values are 1.595 (3) and 1.618 (3) Å, respectively.

The most interesting structural feature of the P_2SN_3 ring is the variation in P–N bond lengths. The mean P–N bond length in the PNP units is ca. 1.580–1.596 Å for all four derivatives, a value

(26) Krishnamurthy, S. S.; Sau, A. C.; Woods, M. *Adv. Inorg. Chem. Radiochem.* **1978**, *21*, 41.
(27) Purcell, J. F.; Kotz, J. C. "Inorganic Chemistry"; W. B. Saunders: Philadelphia, 1977.
(28) Olsen, F. P.; Barrick, J. C. *Inorg. Chem.* **1973**, *12*, 1353.

Table IV. Positional Parameters (×10⁴) and B_{eq} (×10) for the Non-Hydrogen Atoms of $(Ph_2PN)_2(NSNMe_2)$

atom	x/a	y/b	z/c	B_{eq}, Å²
S	−1887.6 (8)	1847.7 (9)	3953.2 (3)	36
P(1)	−117.4 (8)	2467.6 (9)	3122.9 (3)	33
P(2)	963.0 (8)	1499.4 (9)	4041.2 (3)	32
N(1)	−1587 (2)	2273 (3)	3373 (1)	38
N(2)	1163 (2)	2115 (3)	3475 (1)	34
N(3)	−542 (2)	1444 (3)	4266 (1)	35
N(4)	−2777 (3)	370 (3)	3870 (1)	43
C(1)	−2047 (4)	−739 (4)	3611 (1)	65
C(2)	−3365 (4)	−42 (5)	4354 (2)	80
C(11)	−78 (3)	1446 (3)	2543 (1)	30
C(12)	−1256 (3)	1174 (4)	2274 (1)	45
C(13)	−1256 (4)	331 (4)	1841 (1)	54
C(14)	−73 (4)	−254 (4)	1677 (1)	49
C(15)	1111 (4)	−2 (4)	1937 (1)	48
C(16)	1102 (3)	857 (4)	2367 (1)	40
C(21)	6 (3)	4261 (3)	2930 (1)	31
C(22)	285 (4)	5232 (4)	3317 (1)	45
C(23)	309 (3)	6642 (4)	3206 (1)	53
C(24)	66 (3)	7084 (4)	2711 (1)	52
C(25)	−198 (4)	6147 (4)	2325 (1)	49
C(26)	−230 (3)	4736 (4)	2438 (1)	41
C(31)	1929 (3)	2510 (3)	4501 (1)	33
C(32)	3326 (4)	2512 (4)	4486 (1)	46
C(33)	4071 (4)	3237 (4)	4846 (2)	60
C(34)	3418 (5)	3976 (5)	5228 (2)	64
C(35)	2050 (4)	3996 (4)	5243 (2)	65
C(36)	1300 (3)	3262 (4)	4882 (1)	51
C(41)	1765 (3)	−186 (3)	4075 (1)	31
C(42)	1484 (3)	−1077 (4)	4480 (1)	43
C(43)	2143 (4)	−2342 (4)	4518 (1)	49
C(44)	3055 (4)	−2727 (4)	4155 (1)	47
C(45)	3353 (4)	−1851 (4)	3749 (1)	47
C(46)	2703 (3)	−585 (4)	3710 (1)	40

that is typical for cyclophosphazenes [cf. 1.576 (6) Å for $(Ph_2PN)_3$].[29] In contrast, the mean P–N bond length in the PNS unit is significantly longer in **5a** and **5b** at 1.667 (5) and 1.662 (9) Å, respectively. The difference is less pronounced for **5d** in which d(P–N(S)) is 1.618 (2) Å, and it is almost negligible for **5c**, d(P–N(S)) = 1.606 (2) Å.

In a preliminary communication, we suggested that these differences indicate a tendency toward localization of π bonding at opposite ends of the molecule,[11] implying that π bonding is weakest in the P–N bonds connecting the PNP and NSN units. The new structural data for **5c** and **5d** indicate that the polarization of π bonding is much less pronounced for the less electronegative Ph substituent and absent for the electron-releasing Me_2N substituent, which imposes equal P–N bond lengths and planarity for the P_2SN_3 ring. In order to understand these structural features of the $P_2SN_3^+$ ring and the tendency for ring-opening reactions to occur, we have carried out simple Hückel and ab initio HFS SCF MO calculations to determine the electronic structure of the $P_2SN_3^+$ ring (**2**) and to compare it with the related six-membered rings P_3N_3 (**1**), PS_2N_3 (**3**), and $S_3N_3^-$ (**4**).

Electronic Structure and Bonding in the $P_2SN_3^+$ Ring—Simple Hückel Calculations. Some useful insight into the π-electronic structure of PSN rings can be gained from simple Hückel calculations.[30] The ring systems PS_2N_3 and $P_2SN_3^+$ can be viewed as single-atom substitutions of the $S_3N_3^-$ and P_3N_3 rings, respectively. The former involves the replacement of sulfur in $S_3N_3^-$ by phosphorus (formally R_2P^+), while the substitution of S^+ for P in P_3N_3 yields $P_2SN_3^+$. We have shown previously that the interaction of the $S_2N_3^-$ unit in PS_2N_3 with the relatively high-energy d orbitals on phosphorus effects a general stabilization of the π MOs of the thiazene unit, but the ring retains many of the structural and electronic features of that unit.[8] In contrast, incorporation of a sulfur center into the phosphazene $P_2N_3^-$ moiety results in more profound adjustments to the electronic structure

(29) Ahmed, F. R.; singh, P.; Barnes, W. H. *Acta Crystallogr., Sect. B: Struct. Crystallogr. Cryst. Chem.* **1969**, *B25*, 316.
(30) Burford, N. Ph.D. Thesis, University of Calgary, 1983.

Table V. Positional Parameters (×10⁴) and B_{eq} (×10) for the Non-Hydrogen Atoms of $(Ph_2PN)_2(NSPh)$

atom	x/a	y/b	z/c	B_{eq}, Å²
S	2958.4 (3)	2188.2 (5)	1948.4 (5)	48
P1	3153.7 (3)	4127.9 (5)	1849.1 (4)	43
P2	1920.1 (3)	3480.9 (5)	1501.4 (5)	43
N(1)	3320 (1)	3030 (1)	1759 (2)	50
N(2)	2490 (1)	4288 (1)	1849 (1)	46
N(3)	2167 (1)	2391 (1)	1565 (1)	47
C(1)	3364 (1)	2203 (2)	3070 (2)	47
C(2)	4048 (1)	2391 (2)	3580 (2)	57
C(3)	4377 (2)	2298 (2)	4431 (2)	60
C(4)	4032 (2)	2014 (2)	4775 (2)	65
C(5)	3357 (2)	1815 (3)	4271 (3)	74
C(6)	3020 (2)	1899 (2)	3420 (2)	59
C(11)	3129 (1)	4764 (2)	1017 (2)	42
C(12)	2993 (1)	4292 (2)	305 (2)	55
C(13)	2972 (2)	4787 (3)	−326 (2)	66
C(14)	3068 (2)	5753 (3)	−273 (2)	63
C(15)	3193 (2)	6225 (2)	422 (2)	62
C(16)	3226 (1)	5742 (2)	1061 (2)	53
C(21)	3839 (1)	4687 (2)	2775 (2)	42
C(22)	3741 (1)	5205 (2)	3309 (2)	49
C(23)	4283 (2)	5642 (2)	4005 (2)	57
C(24)	4916 (2)	5568 (2)	4167 (2)	56
C(25)	5022 (2)	5048 (3)	3648 (2)	67
C(26)	4485 (1)	4605 (3)	2953 (2)	65
C(31)	1514 (1)	3628 (2)	2057 (2)	42
C(32)	1593 (1)	4449 (2)	2490 (2)	58
C(33)	1291 (2)	4548 (3)	2926 (2)	70
C(34)	914 (2)	3824 (3)	2934 (2)	72
C(35)	828 (2)	3010 (3)	2509 (3)	89
C(36)	1122 (2)	2906 (2)	2061 (2)	71
C(41)	1271 (1)	3675 (2)	414 (2)	46
C(42)	849 (2)	4465 (2)	157 (2)	54
C(43)	385 (2)	4645 (2)	−677 (2)	61
C(44)	345 (2)	4047 (3)	−1264 (2)	68
C(45)	755 (2)	3269 (3)	−1026 (2)	78
C(46)	1211 (2)	3083 (2)	−199 (2)	66

Table VI. Selected Bond Lengths (Å) and Bond Angles (deg) for $(Ph_2PN)_2(NSX)$ (X = Cl, I, NMe_2, Ph)

	X			
	Cl (**5a**)	I (**5b**)	NMe_2 (**5c**)	Ph (**5d**)
S–N(1)	1.556 (4)	1.556 (7)	1.586 (3)	1.615 (3)
S–N(3)	1.552 (4)	1.544 (7)	1.603 (2)	1.621 (2)
P(1)–N(2)	1.581 (4)	1.590 (7)	1.595 (2)	1.594 (3)
P(2)–N(2)	1.578 (4)	1.582 (7)	1.593 (2)	1.598 (2)
P(1)–N(1)	1.660 (5)	1.667 (9)	1.608 (2)	1.621 (2)
P(2)–N(3)	1.674 (5)	1.656 (9)	1.604 (2)	1.616 (2)
S–X	2.357 (2)	2.713 (3)	1.685 (3)	1.810 (3)
N(1)–S–N(3)	117.6 (2)	116.8 (4)	112.4 (1)	113.5 (1)
S–N(1)–P(1)	121.3 (2)	121.5 (5)	125.8 (1)	118.4 (2)
P(1)–N(2)–P(2)	125.6 (3)	124.8 (3)	120.2 (1)	120.7 (1)
P(2)–N(3)–S	121.3 (2)	122.5 (5)	125.5 (1)	118.8 (1)
N(1)–P(1)–N(2)	115.2 (2)	115.7 (3)	117.7 (1)	115.7 (1)
N(2)–P(2)–N(3)	113.7 (2)	114.3 (3)	117.7 (1)	116.6 (1)
dihedral angle[a]	93.0	95.3	121.0	98.4

[a] Angle between the S–X vector and the NPNPN plane.

Table VII. Best Planes for $(Ph_2PN)_2(NSX)$ (X = Cl, I, NMe_2, Ph)

	X			
	Cl (**5a**)	I (**5b**)	NMe_2 (**5c**)	Ph (**5d**)
N(1)	0.04	0.05	−0.02	−0.03
P(1)	−0.05	−0.05	0.01	−0.03
N(2)	0.02	0.01	0.03	0.13
P(2)	0.02	0.03	−0.05	−0.15
N(3)	−0.03	−0.04	0.03	0.09
S	0.30	0.29	0.08	0.55

of the ring since the energy of the π-type orbital on sulfur is *intermediate* between the energies of the two groups of π MOs

Table VIII. Eigenvalues and Mulliken Population Analysis for Planar $(H_2PN)_2(SN)^+$

orbital designation	eigenvalues, au	overlap population				centers				
		SN_a	PN_a	PN_b	PH	S	N_a	N_b	P	H
$1a_1$	−1.099	0.064	0.020	0.008	0.000	0.16	0.17	0.04	0.02	0.00
$1b_2$	−0.997	−0.034	−0.044	0.001	0.000	0.04	0.29	0.00	0.04	0.00
$2a_1$	−0.995	0.018	−0.003	0.070	0.001	0.08	0.02	0.42	0.06	0.00
$3a_1$	−0.813	−0.019	−0.065	−0.006	0.003	0.31	0.13	0.13	0.09	0.00
$2b_2$	−0.810	0.028	−0.006	0.030	0.011	0.06	0.08	0.06	0.22	0.01
$3b_2$	−0.667	0.020	0.031	0.032	0.002	0.11	0.14	0.12	0.10	0.00
$4a_1$	−0.661	−0.019	−0.013	−0.009	0.030	0.19	0.05	0.04	0.25	0.02
$1b_1$	−0.614	0.014	0.017	0.016	0.021	0.07	0.05	0.04	0.13	0.02
$1a_2$	−0.575	0.002	0.016	0.000	0.040	0.00	0.03	0.00	0.22	0.04
$4b_2$	−0.557	0.002	0.006	0.018	0.025	0.01	0.03	0.18	0.22	0.02
$5a_1$	−0.548	−0.001	0.005	−0.006	0.003	0.21	0.27	0.09	0.03	0.00
$2b_1$	−0.541	0.043	−0.008	0.009	0.013	0.38	0.09	0.03	0.06	0.01
$6a_1$	−0.506	−0.043	−0.026	0.017	0.001	0.56	0.04	0.05	0.09	0.00
$5b_2$	−0.439	−0.002	0.015	0.002	0.002	0.03	0.41	0.04	0.03	0.00
$2a_2$	−0.439	0.025	0.012	0.000	0.009	0.02	0.34	0.00	0.02	0.02
$7a_1$	−0.423	−0.022	−0.003	0.018	0.001	0.15	0.17	0.46	0.03	0.00
$3b_1$	−0.402	−0.001	0.001	0.047	0.012	0.00	0.00	0.51	0.04	0.04
$4b_1$	−0.317	−0.090	0.038	−0.001	−0.004	0.67	0.24	0.00	0.04	0.02
total π		0.33	0.15	0.29	0.38					
total σ		0.25	0.53	0.71	0.31					
total		0.58	0.68	1.00	0.69					

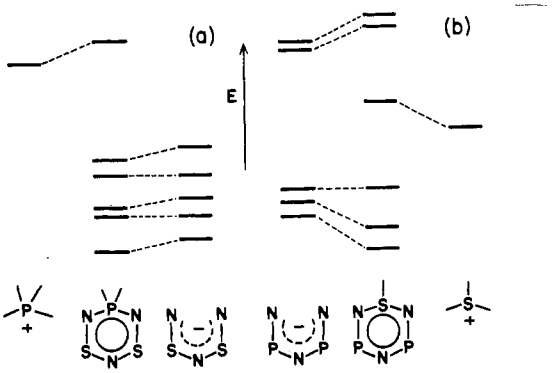

Figure 2. Single-atom perturbation of (a) the π system of $S_2N_3^-$ by a phosphorus oribtal and (b) the π system of $P_2N_3^-$ by a sulfur orbital.

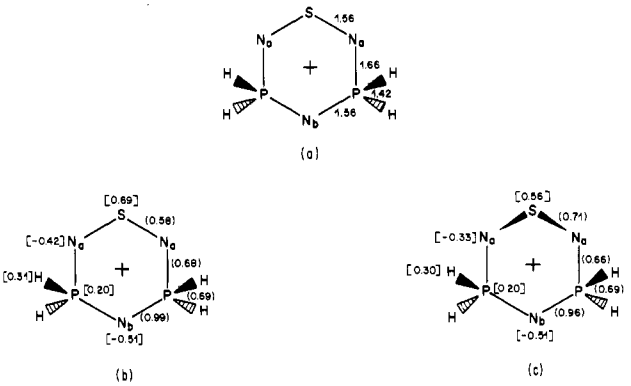

Figure 3. (a) Bond lengths (Å) for planar $(H_2PN)_2(SN)^+$. (b, c) Charges (in brackets) and total overlap populations (in parentheses) for (b) planar and (c) half-chair conformations (S atom is 0.31 Å out of plane) of $(H_2PN)_2(SN)^+$.

of the phosphazene unit (Figure 2). The interaction results in a stabilization of the lower nitrogen-based orbitals and a destabilization of the upper phosphorus-based orbitals. Consequently, variations in bond lengths around the ring are expected to be greater than in the perturbed thiazene.[31]

In the molecule $(Ph_2PN)_2(NSX)$, one electron in the P_2SN_3 system is presumed to be associated with the ligand X and the species of interest is taken to be the $P_2SN_3^+$ cation. The HMO calculations for the 6-π-electron $P_2SN_3^+$ ring show that the three occupied energy levels (in order of increasing energy) are a strongly bonding MO with respect to the NSN segment of the ring, a strongly bonding MO with respect to the PNP unit, and a nonbonding MO located on the equivalent nitrogen atoms. The LUMO is a π^* MO based mainly on sulfur and *strongly antibonding with respect to the S–N bonds*. Thus, the simple HMO approach provides a basis for rationalizing both the inequalities in P–N bond lengths and the facile ring-opening reactions (with S–N bond rupture) of the $P_2SN_3^+$ ring.

Ab Initio MO Calculations. In order to gain a more detailed understanding of the electronic structure of this heterocycle and to compare it with the results for the related six-membered rings P_3N_3, PS_2N_3, and $S_3N_3^-$, we have also carried out ab initio HFS SCF calculations. For ease of calculation the substituents on phosphorus were taken to be hydrogen, cf. $(H_2PN)(SN)_2$.[8] The calculations were carried out for the planar ring, $(H_2PN)_2(SN)^+$,[32] as well as for a $P_2SN_3^+$ ring in which the sulfur is lifted out of the plane by 0.31 Å by the bond lengths indicated in Figure 3a. The total overlap populations and atomic charges for the planar (C_{2v}) and nonplanar (C_s) molecules are compared in Figure 3b,c. The calculated charges indicate highly polar bonds. Indeed, the S–N bonds are more polar than in $S_4N_4^{2+}$ (where $q_N = -0.19$ and $q_S = 0.69$),[16b] but the P–N bonds are less polar than in $(H_2PN)(SN)_2$ (where $q_N = -0.51$ and $q_P = 0.29$).[8] A less polar S–N bond results when sulfur is lifted out of the plane of the other five atoms (Figure 3c).

The total overlap populations suggest a double P–N bond (0.99, 0.96) in the PNP unit and a strong single bond (0.68, 0.66) for the "connecting" P–N bonds, consistent with the bond inequalities observed for **5a** and **5b**. The S–N overlap population of 0.58 is larger than that found in most sulfur–nitrogen molecules (cf. 0.45–0.52 in $S_4N_5^+$)[33] and is comparable to that found in $S_4N_4^{2+}$ (0.61).[16b] Although the S–N bond is the weakest cyclic bond, on the basis of overlap populations, it is strengthened significantly when the sulfur is lifted out of the plane (0.71). The energies of the two ring conformations are, however, the same to the limit of the accuracy of our methods (ca. 5 kcal).

(31) Variations in endocyclic bond lengths in geminally substituted cyclophosphazenes, e.g. *gem*-$Me_2F_6P_4N_4$, have been ascribed to the π-inductive effect of the geminal substituents: Marsh, W. C.; Ranganathan, T. N.; Trotter, J.; Paddock, N. L. *J. Chem. Soc. A* **1971**, 573.

(32) A planar geometry has been reported for the cation $(Cl_2PN)_2(SN)^+$.[13] In this investigation we attempted to determine the X-ray crystal structure of $(Ph_2PN)_2(SN)^+Br_3^-$[17] but were unable to solve it. Crystal data: tetragonal, point group $P422$, $a = 12.8131$ (5) Å, $c = 32.4333$ (24) Å, $Z = 8$, $V = 5319$ Å^3, $D_{calcd} = 1.71$ g cm^{-3}.

(33) Chivers, T.; Fielding, L.; Laidlaw, W. G.; Trsic, M. *Inorg. Chem.* **1979**, *18*, 3379.

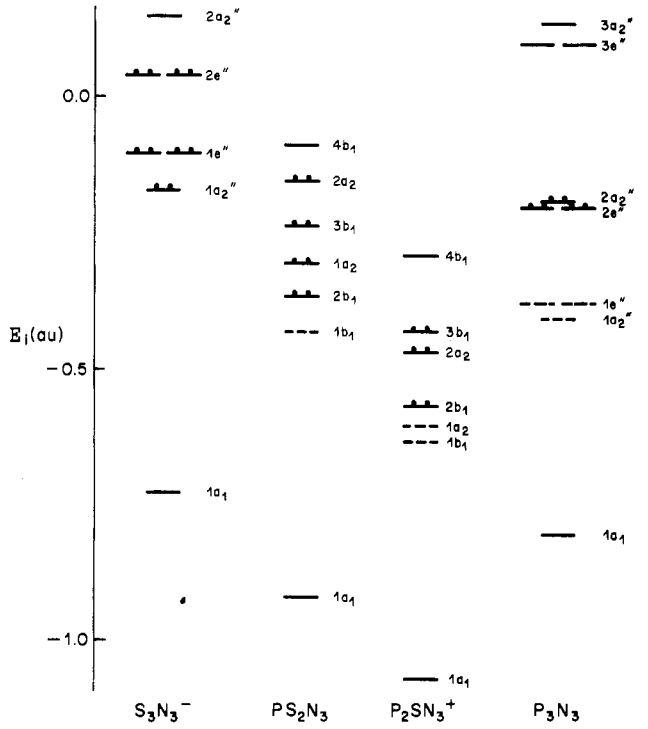

Figure 4. Comparison of the π MO energy levels for $(H_2PN)_3$, $(H_2PN)_2(SN)^+$, $(H_2PN)(SN)_2$, and $S_3N_3^-$ showing the occupancy of the endocyclic π MOs. The dashed lines represent the (occupied) π PH_2 MOs. The lowest occupied molecular orbitals ($1a_1$, LOMO) are also included.

Table IX. 1s Hydrogen Population in MOs of $(H_2PN)_2(SN)^+$

σ orbitals				π orbitals			
$1a_1$	0.000	$1b_2$	0.001	$1a_2$	0.154	$1b_1$	0.088
$2a_1$	0.004	$2b_2$	0.039	$2a_2$	0.050	$2b_1$	0.050
$3a_1$	0.010	$3b_2$	0.006			$3b_1$	0.084
$4a_1$	0.092	$4b_2$	0.086				
$5a_1$	0.010	$5b_2$	0.004				
$6a_1$	0.006						
$7a_1$	0.006						

σ population = 0.26 π population = 0.43

The MOs can be partitioned into two sets, π and σ.[34] The former refers to orbitals that are antisymmetric, and the latter comprises those that are symmetric with respect to the molecular plane. For the symmetry group C_{2v} these sets are a_1, b_2 for σ and a_2, b_1 for π. In Figure 4, the MO energy levels of $P_2SN_3^+$ are compared with those of the P_3N_3, PS_2N_3, and $S_3N_3^-$ rings. The bond overlap populations and self-atom populations for the individual orbitals of $P_2SN_3^+$ are provided in Table VIII. The use of the 1s hydrogen atomic orbitals in the MOs is given in Table IX.

π System in $P_2SN_3^+$. There are five occupied MOs of π symmetry: $1a_2$, $2a_2$, $1b_1$, $2b_1$, and $3b_1$. The atomic orbital populations (Table IX) indicate 0.43 electron from each hydrogen is involved in π orbitals. Thus, approximately one hydrogen electron is involved in each PH_2 π orbital. Assuming that phosphorus also contributes one electron to each PH_2 π orbital, then a total of four π electrons are to be associated with the two PH_2 groups *leaving six π electrons for the cyclic system.* This is analogous to the situation in $(H_2PN)(SN)_2$ where two of the 10 π electrons could be associated with the PH_2 group leaving eight cyclic π electrons.[8] However, the classification of the individual π orbitals into cyclic and exocyclic PH_2 components is more difficult for $(H_2PN)_2(SN)^+$ than for $(H_2PN)(SN)_2$. Certainly both the atomic population (0.22) and the overlap population (0.040) suggest that $1a_2$ is primarily a PH_2 orbital whereas $2a_2$ is mainly a cyclic π orbital. On the other hand the 1s hydrogen population (Table IX) is more evenly distributed among the b_1 orbitals (0.09, 0.05, 0.08) as is the P–H overlap population (0.021, 0.013, 0.012). However, it is clear from the P–N and S–N overlap populations in Table VIII that $2b_1$ and $3b_1$ are the principal contributors to cyclic π character. Consequently, in a somewhat oversimplified picture, we can view $2b_1$, $2a_2$, and $3b_1$ as the cyclic π orbitals.

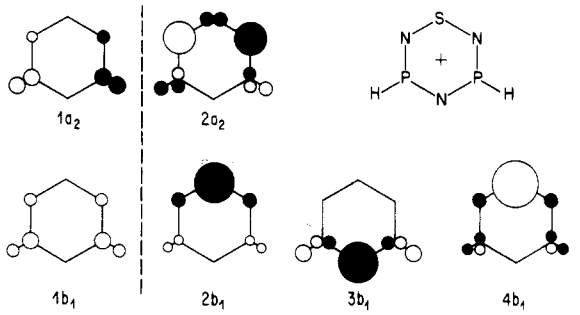

Figure 5. Composition of the endocyclic [$2b_1$, $2a_2$, $3b_1$ (HOMO), $4b_1$ (LUMO)] and PH_2 π MOs of $(H_2PN)_2(SN)^+$. Only one of the two exocyclic hydrogens is shown in this view from above the molecule.

The character of the cyclic π orbitals suggests that the π system can by analyzed in terms of the interaction of the π systems of the fragments, PNP^+ and NSN (Figure 5). For example, the lowest two, $2b_1$ and $2a_2$, are localized on the NSN unit and certainly display the features of the two lowest orbitals of a three-center NSN π system [i.e., $2b_1$ is bonding throughout NSN and $2a_2$ is primarily a nitrogen-centered lone pair orbital (1p)].[35] As a result, the π component of the NSN bonds is only a partial π bond as reflected by the S-N π-overlap population of 0.33 (a full π bond is about 0.5). The HOMO, $3b_1$, is localized on the PNP region of the ring and is largely responsible for the π bonding over these three centers. The overlap population of 0.29 indicates only a partial π bond for these P–N bonds. The π-overlap population (0.15) for the connecting P–N bonds (of the PNS units) arises from small contributions from all π orbitals and suggests a very weak π bond. The existence of weak connecting bonds is reminiscent of the situation in the related six-membered ring S_4N_2 for which a two-fragment approach (NSN, SSS) proved useful in the description of the electronic structure.[36] In summary then, the gross π-electronic structure of the $P_2SN_3^+$ ring can be described as π_{NSN}^2, π_{lpN}^2, π_{PNP}^2, a pattern that is the expected result of the weak interaction of a four-π-electron NSN unit with a higher energy two-π-electron $H_2PN^+PH_2$ fragment.

It should be recalled that the facile ring-opening reactions observed for the $P_2SN_3^+$ occur via cleavage of S–N and not the connecting P–N bonds.[14,15] Table VIII and Figure 5 show that the LUMO, $4b_1$, for $P_2SN_3^+$ is very strongly antibonding with respect to the NSN segment of the ring and weakly bonding with respect to the P–N(S) bonds. The reagents that have been observed to induce rupture of the $P_2SN_3^+$ ring are either nucleophiles or reducing agents. These reagents can be expected to function via partial occupation of the LUMO leading to a substantial weakening of the S–N framework bonds.

The P_2SN_3 ring in **5c** is planar (vide supra), and the S–N overlap populations indicate weaker S–N bonds than in the half-chair conformation. There is little indication, however, of π bonding between the exocyclic Me_2N substituent and sulfur. Indeed in this case donation of π electrons from the dimethylamino group jeopardizes the usefulness of the cation model used in this discussion. For example, strong π bonding of the Me_2N group would produce a new π network that, if localized on the NS-

(34) The use of π symmetry normally involves a plane of symmetry containing the nuclei. In the present case the hydrogen atoms are located symmetrically with reference to the plane containing the P, S, and N centers. The spherical s type distributions on the hydrogens can and do participate in the π- and σ-symmetry molecular orbitals.

(35) Laidlaw, W. G.; Trsic, M. *Inorg. Chem.* **1981**, *20*, 1792.
(36) Chivers, T.; Codding, P. W.; Laidlaw, W. G.; Liblong, S. W.; Oakley, R. T.; Trsic, M. *J. Am. Chem. Soc.* **1983**, *105*, 1186.

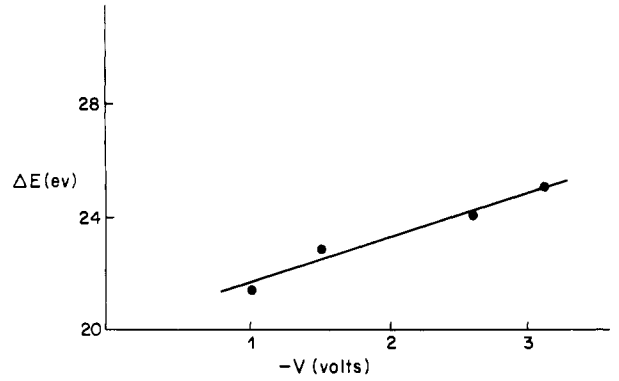

Figure 6. $\Delta[\epsilon(\pi$ LUMO) $- \epsilon$(LOMO)] vs. $E_{1/2}$ (polarographic half-wave reduction potentials vs. Ag/0.1 M Ag^+) for $(Ph_2PN)_2(SN)^+$, $(Ph_2PN)(SN)_2$, $S_3N_3^-$, and $(Ph_2PN)_3$.

$(NMe_2)N$ region of the ring, would generate a bonding orbital distributed over all three S–N bonds and two nonbonding orbitals on the nitrogens weakening, more or less equally, all three S–N bonds. However, donation of two π electrons would generate $P_2SN_3^-$ and result, to a first approximation, in occupation of the NSN antibonding orbital. It is interesting to note that **5c** undergoes a ring-opening reaction at 23 °C in acetonitrile to give a 12-membered ring.[14]

σ System in $P_2SN_3^+$. The separation of the σ orbitals into cyclic and exocyclic PH_2 orbitals is more straightforward, and both the hydrogen 1s populations (Table IX) and the overlap populations (Table VIII) indicate that $4a_1$ and $4b_2$ generate the exocyclic σ bonds for the two PH_2 groups. The remaining σ orbitals are associated with the ring, and from the overlap populations (Table VIII), it can be seen that $1a_1$, $2a_1$, $3a_1$, $1b_2$, $2b_2$, and $3b_2$ are largely σ bonding throughout the ring. The orbitals $5a_1$ and $5b_2$ are lone pairs, principally on nitrogen, whereas $6a_1$ and $7a_1$ have strong S–N antibonding character. The total σ-overlap population of 0.53 for the P–N(S) bonds (Table VIII) indicates a full σ bond whereas the larger value of 0.71 for the P–N(P) bonds results from both sp overlap along the line of centers (as in $2a_1$) as well as "in-plane" pd overlap (as in $3b_2$). The small σ-overlap population of 0.26 for the S–N bonds is typical of cyclothiazenes and reflects the fact that the occupied antibonding orbitals (e.g., $6a_1$) are strongly localized in the S–N region and offset the bonding contributions of the orbitals $1a_1$ etc. The nitrogen lone pairs $5a_1$ and $5b_2$ are well localized and consequently do not make a significant contribution to the bonding. In summary, we have a ca. 1.5 σ bond for each P–N(P) link, a single σ bond for P–N(S), and a ca. 0.5 σ bond for each S–N bond.

Charge Distribution and Hybridization Scheme. Partitioning of atomic populations into σ and π contributions provides some insight into the redistribution of charge in $P_2SN_3^+$. For example, the σ and π charges averaged for the nitrogens are 4.14 and 1.28, respectively. Assuming an atomic hybridization $(sp^2)_\sigma^4(p)_\pi^1$ this means that about two-thirds of the excess population is carried by the π network (i.e., 1.28 – 1.0 = 0.28) whereas only about one-third is carried by the σ system (i.e., 4.14 – 4.0 = 0.14). In the case of sulfur the σ and π populations are 4.01 and 1.30, respectively. Taking the hybridization of sulfur as $(sp^2)_\sigma^4(p)_\pi^2$, these numbers indicate that the deficiency in electron density of 0.69 is brought about solely by loss of π electrons. The analysis for phosphorus is less straightforward. The σ population is 3.23 while the π-symmetry orbitals contain a population of 1.56. As pointed out earlier, the latter number also includes the exocyclic PH_2 π bond. If one assumes that a full electron from this "π population" should be assigned to the exocyclic PH_2 π bond, this leaves only 1.56 – 1.0 = 0.56 cyclic π electrons and increases the σ plus exocyclic charge to 4.23. In terms of this analysis and an atomic hybridization of $(sp^3)_\sigma^4(d)_\pi^1$, phosphorus has lost 0.44 electron to the cyclic π system and gained 0.23 electron from the rest of the orbitals.

The hybridization of phosphorus and sulfur in the $P_2SN_3^+$ cation is also of interest, and some insight can be obtained by analysis of the atomic orbital populations. Following the procedure described in detail for PS_2N_3,[8] one finds that the d orbitals of phosphorus are heavily involved in the π network as they are to a lesser extent for sulfur (Figure 5).

Electrochemical Reduction. The molecular orbital diagram for $P_2SN_3^+$ (Figure 4) indicates that the exocyclic phosphorus bonds (PH_2 in our model) are buried in the stack and, consequently, do not enter an analysis of the frontier orbitals. Although not as clear cut in $P_2SN_3^+$ as in PS_2N_3, they have little effect on the cyclic π manifold. The algebraic value of the eigenvalues depicted in Figure 4 shows the expected decrease from anion to neutral molecule to cation (for $S_3N_3^-$, PS_2N_3, and $P_2SN_3^+$, respectively) and an associated decrease in the energy of the LUMO. This trend is consistent with the polarographic reduction potentials found for this series ($E_{1/2}$ vs. Ag/0.1 M $AgClO_4$ = –2.6 V for $S_3N_3^-$, –1.5 V for PS_2N_3, and –1.0 V for $P_2SN_3^+$). Perhaps of more interest is the observation that the calculated value of the LUMO for P_3N_3 is consistent with a substantial increase in the reduction potential ($E_{1/2}$ = –3.1 V) compared to the mixed P/S–N rings.[37] In the comparison of anions, cations, and neutral species some account of the charge-related shift in eigenvalues must be attempted. By subtracting the energy of the lowest occupied molecular orbital (LOMO), one provides a common reference.[33] The correlation of $\Delta = \epsilon(\pi$ LUMO) $- \epsilon$(LOMO) vs. reduction potential is depicted in Figure 6 for the HFS calculations. A similar correlation is obtained from energies calculated by the simple Hückel method.

UV–Visible Spectrum. The three lowest energy symmetry-allowed transitions for $P_2SN_3^+$ are $3b_1 \rightarrow 4b_1$, $7a_1 \rightarrow 4b_1$, and $2a_2 \rightarrow 4b_1$. From the transition state method,[38] the λ_{max} for these transitions are calculated to be 224, 300, and 315 nm, respectively. The UV–visible absorption spectrum of $(Ph_2PN)_2(NSCl)$ (**5a**) (1×10^{-4} M in MeCN) shows a weak shoulder at 292 nm (ϵ 800 M^{-1} cm^{-1}).[39] Any absorption bands below 280 nm due to the $P_2SN_3^+$ chromophore are obscured by the $\pi \rightarrow \pi^*$ bands of the phenyl substituents on phosphorus.

Conclusion

A comparison of the π electronic structures of the P_3N_3 (**1**), $P_2SN_3^+$ (**2**), PS_2N_3 (**3**) and $S_3N_3^-$ (**4**) rings obtained from ab initio HFS SCF calculations corroborates conclusions based on the idea that the mixed-ring systems **2** and **3** can be viewed as single-atom perturbations of **1** and **4**, respectively. The P–N bond inequalities and the facile S–N bond cleavage observed for **2** can be rationalized from a consideration of the composition of the π MOs. Thus, the highly antibonding S–N nature of the LUMO plays a dominant role in determining the reactivity of this π-electron-precise ring. Similar analyses should be equally informative for other heterocyclothiazenes. The correlation of the energies of the LUMOs of **1–4**, adjusted for the effect of charge, with polarographic reduction potentials suggests a link between theory and experiment in addition to that already established for the electronic excitation energies of sulfur–nitrogen heterocycles.[40]

Acknowledgment. We thank the Natural Sciences and Engineering Research Council of Canada for financial support, Kochi University for a leave of absence (M.H), and Dr. M. N. S. Rao for a sample of $(Ph_2PN)_3$. The HFS MO results were obtained via a program developed by T. Ziegler and J. Baerends.

Registry No. **5a**, 84247-67-6; **5b**, 88008-07-5; **5c**, 88008-11-1; **5d**, 91948-83-3.

Supplementary Material Available: Listings of anisotropic thermal parameters, positional and thermal parameters, distances, angles, and observed and calculated structure factors (90 pages). Ordering information is given on any current masthead page.

(37) The data given here refer to heterocycles with exocyclic Ph groups on phosphorus. An $E_{1/2}$ value of –2.65 V (vs. SCE) for $(Ph_2PN)_3$ has been reported: Allock, H. R.; Birdsell, W. J. *Inorg. Chem.* **1971**, *10*, 2495.
(38) Ziegler, T.; Rauk, A.; Baerends, E. J. *Theor. Chim. Acta* **1977**, *46*, 1.
(39) The height of the anodic polarographic wave due to the oxidation of Cl^- for 10^{-4} M acetonitrile solutions of **5a** indicates that this derivative is completely ionized under such conditions.
(40) Trsic, M.; Laidlaw, W. G. *Int. J. Quantum Chem.: Quantum Chem. Symp.* **1983**, *17*, 367.